STABILITY OF THE BETA PHASE IN Ti-Mo-Cr ALLOY FABRICATED BY POWDER METALLURGY

J. Syarif[a,*], T.N. Rohmannudin[a], M.Z. Omar[a], Z. Sajuri[a], S. Harjanto[b]

[a] Universiti Kebangsaan Malaysia, Faculty of Engineering and Built Environment, Bangi, Malaysia
[b] Universitas Indonesia, Faculty of Engineering, Depok, Indonesia

Abstract

A new β Ti alloy was designed and fabricated by powder metallurgy process using pure metallic powders. The addition of Mo and Cr increased the stability of the β phase. By contrast, O promoted α phase formation upon cooling. The addition of 18%Mo and 10%Cr stabilized the β phase into ambient temperature. O increased the critical cooling rate of formation of α phase due to the prediction of the continuous cooling transformation diagram calculated by the Java-based Material Properties software. Sintering and solution treatment also enhanced the alloying behavior of pure powders to their designated chemical compositions. Hardness of the alloy decreased with increasing Mo and Cr content, which led to the decrease of α phase. The Ti-18%Mo-10%Cr alloy exhibited better corrosion resistance than a commercial Ti-6%Al-4%V alloy, which is used as current biomaterial.

Keywords: Alloying behavior; Oxygen; Critical cooling rate; Hardness; Corrosion resistance; Biomaterials.

1. Introduction

The demand for metallic materials for biomedical devices has grown rapidly in recent years [1]. For example, hip replacements made metallic materials such as titanium and stainless steels are projected to reach 272,000 units by 2030 [1]. Ti alloys have excellent specific strength and corrosion resistance compared with other metallic materials [2]. For this reason, the application of commercial pure (CP) Ti and Ti-6%Al-4%V alloy as implant materials has increased significantly. However, the CP Ti and the Ti-6%Al-4%V alloy suffer from biomechanical incompatibility because of their high elastic modulus (about 120 GPa) compared with human bone (around 30GPa). Therefore, studies on designing β-type Ti alloy, which has low elastic modulus, have focused on the use of Nb, Ta, Zr, and Hf [3-5] owing to their biocompatibility with the human body. Other elements, such as Mo and Cr, have been found to be effective alloying elements for a new β Ti alloy [6]. These elements are β stabilizers and can also increase Mo equivalent [6]. They have been used as implant materials, such as in 304- and 316-stainless steel and in Co-Cr-Mo alloys [7]. Therefore, these elements are potential components for the new β Ti alloy.

The powder metallurgy (PM) process is used to fabricate a new β Ti alloy because it is effective and versatile in producing complex and near net shape components [8]. Products fabricated using this process exhibit properties that are similar to those fabricated using other processes. However, O is picked up as an impurity in the product during the PM process. Thus, O might have a significant effect on the microstructure and mechanical properties of Ti alloys [9].

In this study, a new β-type Ti alloy constituted by Mo and Cr was designed and fabricated through the PM process using pure metallic powders. The effects of Mo, Cr, and O on the phase stability and microstructural change of the alloy were investigated to clarify alloying behavior on sintering. Then, hardness and corrosion resistance were also investigated for the obtained β-Ti alloy.

2. Alloy Design and Experimental Procedures

The stability of the β phase can be predicted by calculating its Mo equivalent [6]. Mo and Cr were the only elements added to the alloy in this work. Thus, we modified the equation as follows: Mo equivalent = 1.00 [Mo] + 1.60 [Cr], where the amount of element is in wt.%. The single β phase can be stabilized into ambient temperature if the case satisfies the following condition: Mo eq. > 10 [10]. Hence, the addition of 5 at.% Mo (equal to 9.8%) or more is almost sufficient in stabilizing β structure to ambient temperature. The other method for designing Ti alloys employs a

---
* Corresponding author: syarif@eng.ukm.my

molecular orbital method, which calculates a bond order *Bo* and a metal d-orbital energy level *Md* [11]. The average values of the *Bo* and the *Md* are generally defined by taking the compositional averages of the parameters; such values are denoted as Bo_{ave} and Md_{ave}, respectively, as shown in the following equations:

$$Bo_{ave} = f_{Ti}.Bo_{Ti} + f_{Mo}.Bo_{Mo} + f_{Cr}.Bo_{Cr}, \qquad ...(1)$$

$$Md_{ave} = f_{Ti}.Md_{Ti} + f_{Mo}.Md_{Mo} + f_{Cr}.Md_{Cr}, \qquad ...(2)$$

where f_{Ti}, f_{Mo}, and f_{Cr} are the atomic fractions of Ti, Mo and Cr, respectively. The values of Bo in the order of Ti, Mo, and Cr were 2.790, 3.063 and 2.779, while those of Md were 2.447, 1.961 and 1.478, respectively.

Calculation of the Bo_{ave} and Md_{ave} values was performed for six types of Ti alloys (†1). The stable phase of the Ti alloy was predicted by plotting Bo_{ave} and Md_{ave} values on a Bo-Md map [11]. Although the Mo equivalent showed that the addition of 9.8% Mo can stabilize the β phase at ambient temperature, the Bo-Md method suggests that the Ti-9.8% Mo alloy would lay on an α+β structure, while other Ti alloys would lay on a single β region.

In this study, commercial pure Ti, Mo, and Cr powders were used as raw materials. All powders were supplied by Alfa Aesar Co (USA). Table 1 shows the purity and particle size of the powders used. The powders were mechanically blended for 3.6 ks. The blended powders were placed in a die cavity with a diameter of 10 mm. These were then consolidated under a pressure of 1000 MPa for 3.6 ks, using a 9-tonne capacity cold press machine at ambient temperature. All samples were subjected to sintering at 1300 °C for 14.4 ks and furnace-cooling. Solution treatment at 1100 °C for 3.6 ks, followed by water-quenching, was carried out for all the samples. Sintering and solution treatment were conducted in an Ar gas atmosphere after achieving vacuumed condition. Microstructures were observed by optical microscopy and scanning electron microscopy (SEM). Samples were etched using a Kroll's reagent. The distribution of elements in the sample was analyzed using SEM-energy-dispersive X-ray spectroscopy (EDS). Phase characterization was evaluated by X-ray diffractratometry (XRD) with Cu-Kα radiation. The concentrations of O and N were measured by NOH gas determinator. Hardness was represented by the average of five measurements in Vickers hardness testing (load 19.6N). Potentiodynamic polarization studies were carried out after 60 s of immersion in Hank's solution for Ti-18%Mo-10%Cr alloy and Ti-6%V-4%Al alloy. Potentiodynamic polarization scans were carried out at a scan rate of 2 mV/ s in the range from –1.0 to 1.0 V vs. SCE. A software package, called Java-based Material Properties (JMatPro), was used to simulate the decomposition of the β phase upon cooling. JMatPro was developed to predict needful material properties using thermodynamic calculation, which integrated various theoretical material models and properties database [12]. The software has been used by many researchers to perform thermodynamic calculations for alloys in equilibrium conditions, such as precipitation [13] and equilibrium phase transformation [14], and also for nonequilibrium conditions, such as time-temperature transformation (TTT) and CCT [15, 16].

Table 1. *Particle size and purity of powders used.*

Element	Particle size/ mesh	Purity /%
Ti	-325	99
Mo	-170	99.5
Cr	-325	99

3. Results and Discussion
3.1 Stability of β phase and alloying behavior

Figure 1 shows the XRD diffractograms of the Ti-Mo alloy. Peaks for the β and other phases were observed in the Ti-Mo alloy although 18%Mo was added to the alloy. Figures 2 show the optical micrographs of the Ti-Mo alloys. Dual-phase structures (i.e., needlelike structures within the matrix) were observed in the samples. Besides the dual-phase structures, pores, which are indicated by arrow signs, are also observed eventhough the samples have been subjected to sintering and solution treatment. Although the Mo equivalent and the Bo-Md method suggested that the single β phase would exist in Ti-18% Mo alloy, β phase was not yet fully stabilized in the Ti-Mo alloys. Pham et al. reported
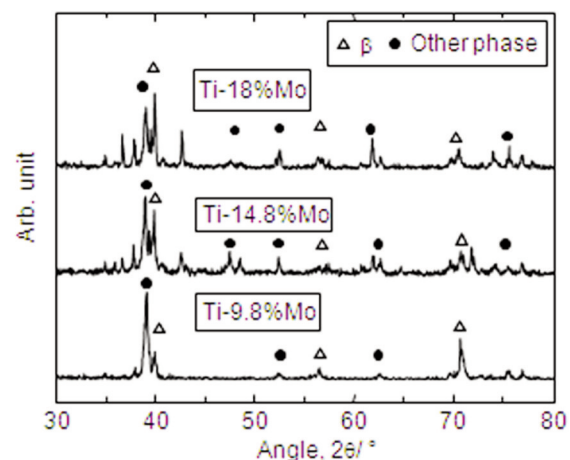

Figure 1. *XRD diffractograms of the Ti-Mo alloys.*

†1 *The six types of alloys were Ti-5at.%Mo, Ti-8at.%Mo, Ti-10at.%Mo, Ti-10at.%Mo-1at%Cr, Ti-10at.%Mo-5at.%Cr, and Ti-10at.%Mo-10at.%Cr. Hereafter, these alloys were expressed in wt.%: Ti-9.8%Mo, Ti-14.8%Mo, Ti-18%Mo, Ti-18%Mo-1%Cr, Ti-18%M0-5%Cr, and Ti-18%Mo-10%Cr.*
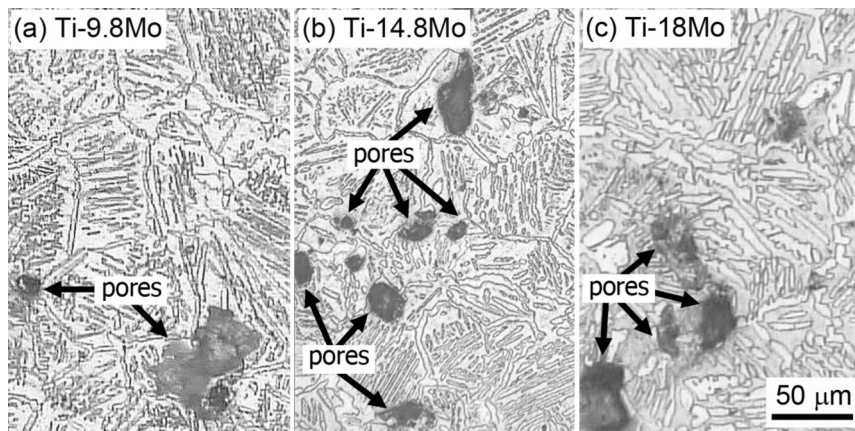
***Figure 2**. Optical micrographs of Ti-Mo alloys.*

that a microstructure, such as the dual-phase structure, can influence the mechanical properties and corrosion resistance of biomedical Ti alloys [17]. Thus, addition of Cr would be effective for stabilizing single β phase into ambient temperature, because the Mo equivalent showed that Cr stabilized the β phase 1.6 fold higher than Mo [6].

Figure 3 shows XRD diffractograms of the ternary Ti-18%Mo-Cr alloy. The single β phase could still not be obtained after the addition of 1%Cr to the Ti-18%Mo alloy. The stability of the β phase increased by adding 5% Cr, but a single β phase was observed in the Ti-18%Mo-10% Cr alloy. Figures 4 shows the optical micrographs of the Ti-18%Mo-Cr alloys. In all samples, pores, which are indicated by the arrow signs, were still observed in all samples. It is found that Ti-18%Mo-1%Cr alloy and Ti-18%Mo-5% alloy still exhibited the dual-phase structures. Finally, an equiaxed structure (i.e., a typical β structure) was obtained in the Ti-18%Mo-10%Cr alloy as shown in Figure 4c. These micrographs correspond well with the XRD difractograms shown in Figure 3. Thus, the addition of 18%Mo and 10%Cr stabilized the single β phase into ambient temperature, and a new single β-phase Ti alloy was successfully obtained.

Meanwhile, Figure 5 shows a backscattered electron image and an elemental mapping measured by EDS for the Ti-18%Mo-10%Cr alloy. As can be seen, all elements were well distributed within the sample. The concentration of each element, measured
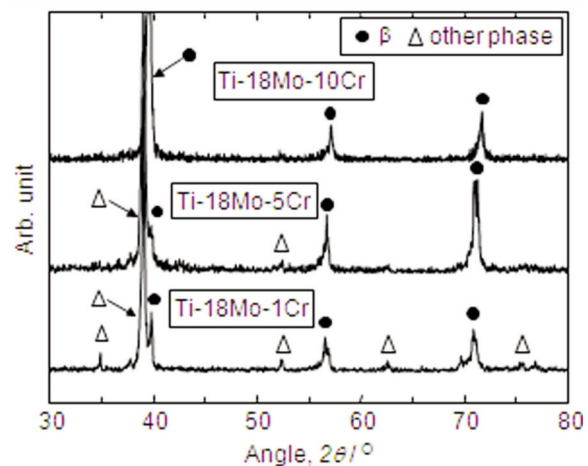

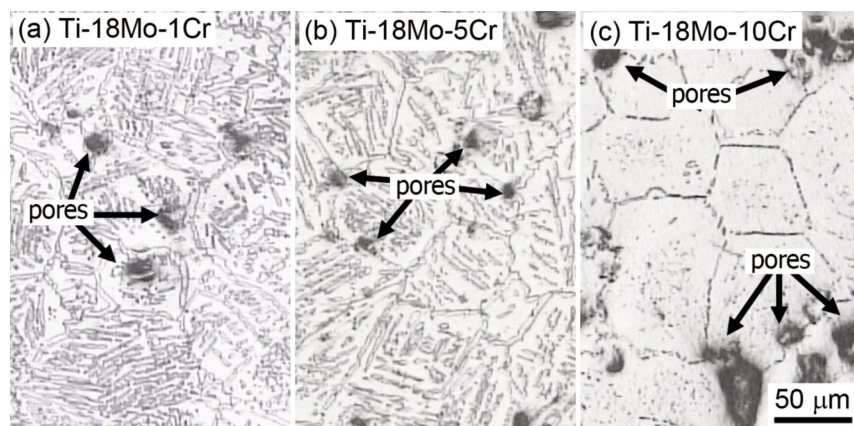***Figure 3**. XRD diffractograms of the Ti-18%Mo-Cr alloys.*

***Figure 4.** Optical micrographs of Ti-18%Mo-Cr alloys.*

by area-mapping mode EDS, is shown in the images close to the designated chemical composition (i.e., 72%Ti-18%Mo-10%Cr). The diffusivity of Cr in the β Ti matrix was four times as high as the self-diffusivity of Ti [18]. Hence, pure Cr powder dissolved easily, and Cr atoms were distributed homogenously in the β matrix of Ti. Mo also reached its designated chemical composition by sintering although the diffusivity of Mo was just one-half that of Ti [18]. Sintering was carried out to enhance interparticle binding among particles. The porosity of Ti-18%Mo-10%Cr alloy was measured by Image-J software, and was found to be around 6 vol.%. From these results, both alloying and interparticle binding of the pure metallic powders were enhanced due to the diffusion of elements. The designated chemical compositions were thus obtained by sintering and solution treatment. The decrease in stability of the β phase was not caused by undissolved metallic powders or alloying elements. Instead, such decrease, as represented by the XRD peak of other phases in Figure 1 and Figure 3, could be due to the formation of martensite (such as α' and α") or the ω phase upon cooling.

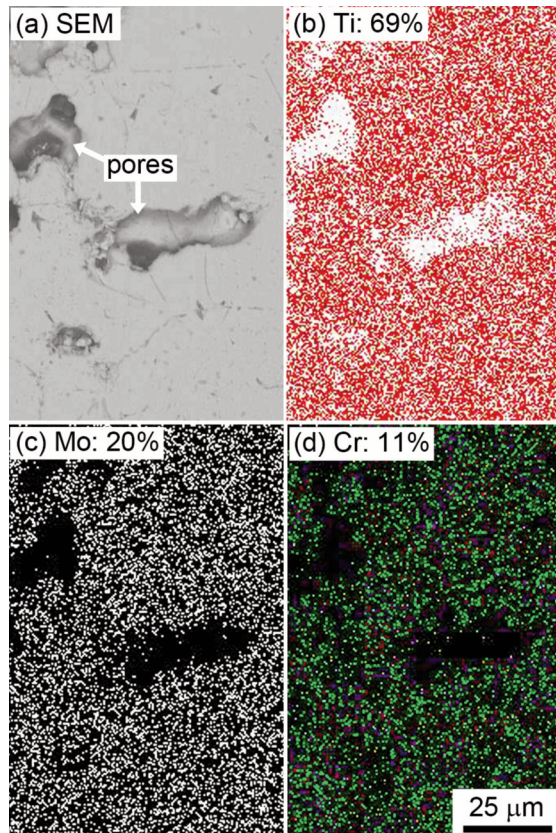Dobromyslov et al. reported that the addition of 5at.%Mo can decrease martensite start (Ms)

Figure 5. *BSE image and elemental mapping of the Ti-18%Mo-10%Cr alloy.*

temperature to 273 K [19]. Min et al. have reported that the formation of the ω phase is suppressed by the addition of 15 mass% Mo [20]. Thus, the decrease in β-phase stability of alloys containing 9.8% Mo (5at.% Mo) Mo or more could not be explained by the formation of martensite and the ω phase. It is indicated that the dual-phase structures as shown in Figure 2 and Figure 4 were not composed by the α', α" or ω phases besides the β phase.

Table 2 represents concentrations of O and N in the Ti-18%Mo-Cr alloy after sintering and solution treatment. The impurity content, especially O, was high in this alloy compared with the O content of the other Ti alloys fabricated by the PM process (up to 0.3wt.%) [21]. Therefore, the concentration of O in the Ti-18%Mo-10%Cr alloy decreased the β phase stability because the impurity is a strong α stabilizer.

Table 2. *Oxygen and nitrogen contaminations in samples.*

Alloy	Oxygen / wt.%	Nitrogen / wt.%
Ti-18%Mo-1%Cr	0.76	0.06
Ti-18%Mo-5%Cr	0.92	0.09
Ti-18%Mo-10%Cr	0.78	0.08

To clarify the effect of O on phase transformation from the β-phase region upon cooling, a continuous cooling transformation was estimated by JMatPro. The calculation for the CCT diagram of the Ti-18%Mo-Cr alloys was carried out by considering the following parameters: soaking temperature was 1000 °C, size of prior β grain was 100 µm, and the formation of 0.5 vol.% of α was defined as a start of β → α transformation (α_s). Figure 6 shows a result of a calculation of the CCT diagram for Ti-18%Mo alloy with 0 wt.% O. As can be seen from the CCT diagrams of both alloys, two types of α phases precipitated from the β phase upon cooling, namely, the α phase along the prior β grain boundaries (GB α) and the α phase in the prior β grain interior (bulk α). The β phase was decomposed into the α phases by a diffusional transformation. No curve for a finish of the β → α transformation (α_f) was estimated by the JMatPro. The critical cooling rates of the formation of the bulk α phase (CCR of bulk α) and the formation of the GB α phase (CCR of GB α) are also superimposed in Figure 6. The CCR of GB α was slower than the CCR of bulk α. Moreover, GB α, bulk α, and β phases were predicted to coexist when the cooling rate was slower than the CCR of the GB α. The combination of the bulk α and β phases was obtained upon moderate cooling, which was lower than the CCR of the bulk α. When the cooling rate was faster than the CCR of the bulk α, then only the β phase existed because the Ms temperature in the alloy was also predicted to be much lower than the ambient temperature.
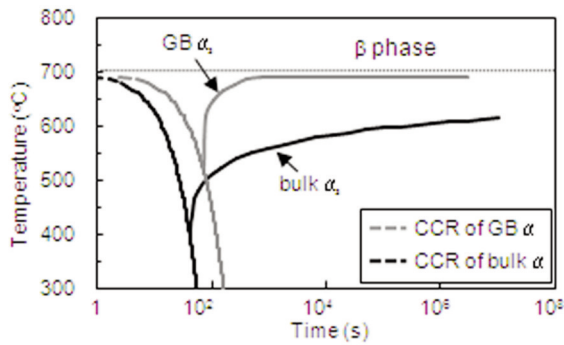
Figure 7 shows the relationship between O

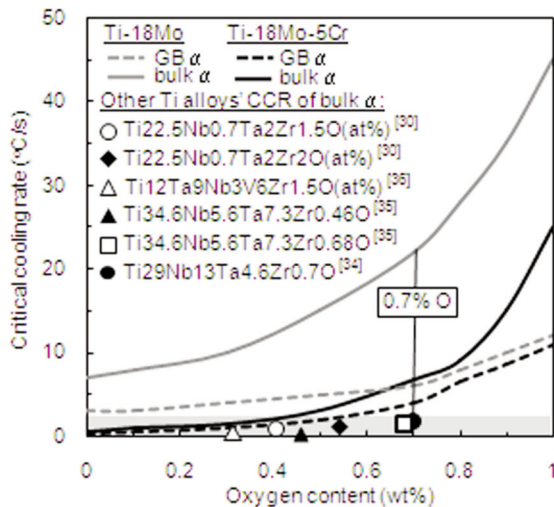**Figure 6.** *CCT diagram of Ti-18%Mo alloy with 0%O.*

Figure 7. *Relation between oxygen content and CCR of Ti alloys.*

concentration and the CCRs of GB α and bulk α of the Ti-18%Mo alloy and the Ti-18%Mo-5%Cr alloy.

As can be seen, all CCRs increased with rising O concentration. The CCR of GB α demonstrated a slight dependence on Cr concentration. The CCR of bulk α exhibited a gradual increase of up to 0.5% O, and then an abrupt increase was observed; this also decreased significantly when 5%Cr was added. This calculation indicated that O significantly influenced the formation of α phase upon cooling, and an increase in Cr concentration retarded the formation of the α phase. For instance, the CCR of bulk α of the Ti-18%Mo-5%Cr alloy with 0.7% O was almost the same as that of the Ti-18%Mo alloy. The CCR of bulk α of the Ti-18%Mo alloy increased threefold due to the addition of 0.7% O. Moreover, the addition of 5%Cr decreased the CCR of bulk α to about one-seventh of the amount for the Ti-18%Mo-0.7%O alloy. Hence, Cr had an inverse proportional relationship with O, although the influence of O was more effective than that of Cr. Therefore, the aforementioned estimation was consistent with the

result, thus revealing an improvement in the β phase of the Ti-18%Mo alloy caused by the addition of Cr (Figures 1 and 3). Furthermore, the aforementioned results also indicated that the dual-phase microstructures, which are observed in Figure 2 and Figure 4, were composed by the the diffusional α phase (i.e., the GB α and the bulk α) and the β phase.

The effects of O and Cr on the change in the β transus can be observed in following equation [22]:

$$\Delta\beta_{tr} \approx -9.5[Mo] - 12.1[Cr] + 123.0[O]. \qquad ...(3)$$

Equation (3) shows that O has a significant effect on the increment of the β transus compared with Cr. For instance, the increment of the β transus was around 86 °C, because of the addition of 0.7% O. Around 7% Cr should be added to set off the effect of 0.7% O. The increase in O content expanded the α+β region and induced the β → α transformation at a relatively elevated temperature within the α+β region. This result indicated that O promoted the formation of α within the α+β region upon cooling. This could be attributed to an increase in the nucleation rate and a promotion of the growth rate of nuclei caused by the increase in the β transus. The nucleation rate is known to be dependent on nucleation energy or the driving force of β → α transformation, which can be estimated by the following relation: 4.0 J/mol x ΔT [23]. The driving force was estimated to be around 20 J/mol by applying supercooling (ΔT) for γ → α transformation of Fe (i.e., 50 °C) [24]. The calculation of the change in Gibb's free energy using the JMatPro for Ti-18%Mo alloy suggested that the change in free energy was around 22.49 J/mol when the alloy was supercooled at 50 °C from the β transus (737 °C). The β transus was shifted to elevated temperatures by O contamination. As a result, supercooling increased along with the applied cooling rate, and β → α transformation was remarkably enhanced.

For O segregation into the β grain boundary, McLean [25], and Seah & Hondros [26] have proposed equations for estimating amount of segregation of impurity. Moreover, Takaki et al. have explained that Seah and Hondros' equation is more accurate for estimating carbon segregation in engineering metals such as C steel [27]. The amount of segregation of impurity proposed by Seah and Hondros is shown in the following equation:

$$(X_{Bo}/X_B)\{X_M/(X_{Mo} - X_M)\} = (1/K) + \{(K-1)/K\}(X_M/X_{Mo}), \qquad ...(4)$$

where X_{BO} is a saturation concentration at the grain boundary, X_B is a concentration at the grain boundary, X_{Mo} is a solubility in the matrix, X_M is a concentration in the matrix, and K is a thermal factor. The value of K is equal to exp (Q/RT) where Q is the thermal energy that shows the difference between the matrix and the grain boundary. The value of Q is 7.32 kJ/mol,

and it is independent from the alloy system. The atomic solubility (X_{MO}) of O in the Ti-18%Mo alloy was predicted to be 0.072 at 1273 K by JMatPro. Although X_{Bo} is unknown, TiO_2 has been reported to be the most stable Ti oxide in the Ti alloy [28]. Thus, X_{Bo} was assumed to be 0.67. X_B was calculated to be around 0.45 (equal to 18.6wt% O) by substituting the values to Equation (4). Therefore, a huge amount of O was suggested to segregate into the β grain boundary. Wu et al. [29] and Wei et al. [30] have also reported that O atoms segregate into the grain boundary of the β phase. The segregation of atom facilitates the formation of nucleation on the grain boundary [31], and O is an α stabilizer; thus, the formation of the α phase can be promoted along the β grain boundary upon cooling. Wu et al. have also reported that the α phase precipitates preferentially along the β grain boundary because of the O segregation in that region [29]. The aforementioned explanations are in good agreement with the finding of the current study. The α phase formation was promoted upon cooling because of the increase in O concentration. In addition, the increase in O was also effective in retarding the formation of the ω phase upon cooling [32].

In contrast to the finding of the present study, Abdel Hady et al. showed that high O levels promote the stability of the β phase into ambient temperature [33]. Ti-29%Nb-13%Ta-4.6%Zr and Ti-34.6%Nb-7.3%Zr-5.6%Ta alloys, which contain 0.7% O, still exhibited the β phase characteristics at ambient temperature [30, 34-36]. To explain the effect of O on the stability of β in the aforementioned alloys, the CCRs of bulk α of the Ti-Nb-Ta-Zr alloys were calculated by JMatPro and plotted in Figure 7. The Ti-Nb-Ta-Zr alloys were found to have very small CCRs of bulk α although the concentration of O was very high in these alloys. The alloys contained high levels of heavy elements such as Nb, Ta, and Zr aside from the high amount of O. Hence, these elements may have induced a solute-drag effect because of their larger atomic radii, possibly retarding the growth of α nuclei during β à α transformation. Tang et al. reported that Nb can reduce the CCR of β → α transformation of Ti alloy upon cooling [37]. The stability of the β phase in the Ti-Nb-Ta-Zr alloy was not promoted by O, but caused by the high concentration of Nb, Ta, and Zr. Mo and Cr in the alloy were relatively low in concentration, and thus could not remarkably lower the CCR. Furthermore, the N in the sample was also believed to influence the promotion of the formation of the α phase upon cooling, although the concentration of N was lower than that of O [38]. The reason is that N is also an α stabilizer and has almost the same Al equivalent with O. Based on the aforementioned result, the single β phase was obtained by adding 18%Mo and 10%Cr and by applying the PM method. The addition of Mo

and Cr increased the stability of the β phase. By contrast, O promoted the formation of the α phase upon cooling. The rise in O content increased CCR for the formation of the α phase. Furthermore, sintering and solution treatment enhanced the alloying behavior of pure metallic powders to their designated chemical compositions.

3.2 Hardness and corrosion resistance of the Ti-18%Mo-10%Cr alloy

Figure 8 represents hardness of the Ti-Mo alloys and Ti-18%Mo-Cr alloys. It is found that the Ti-18%Mo-10%Cr alloy, which consisted of single β phase, exhibited the lowest hardness among other samples. Since the β-grain size of the Ti-18%Mo-10%Cr alloy was quite large, i.e. 100 µm, the hardness of the alloy was dominated by the solid solution hardening of Mo, Cr and O. On the other hand, the hardness of other samples were thought to be controlled by combination of the solid solution hardening of Mo, Cr and O and the precipitation hardening of the α phase. It is because the α phase and the β phase coexisted in the other samples.

It is shown that the hardness of all samples decreased with increasing the concentration of Mo and Cr. The decrease of the hardness might be affected by the decrease of the α phase owing to the addition of Mo and Cr, which could increase the stability of the β phase. Although the contribution of each strengthening mechanism has not been clarified yet, it is suggested that the precipitation strengthening of α phase was predominant than the other strengthening. For instance, the hardness of the Ti-9.8% Mo alloy, which contained the lowest concentration of alloying elements, was 1.5 fold higher than that of the Ti-18%Mo-10%Cr alloy, which had the highest concentration of alloying elements. The aforementioned result suggested that the β Ti-
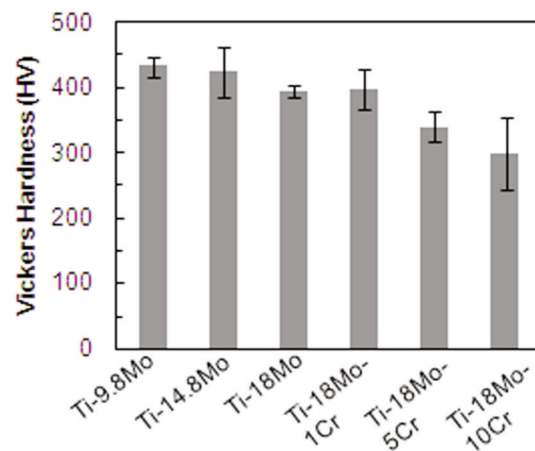
Figure 8. *Hardness of Ti-Mo alloys and Ti-18%Mo-Cr alloys.*

18%Mo-10%Cr alloy had suitable hardness for implant materials because its hardness is almost similar to the hardness of other β Ti alloys such as Ti-8Fe-8Ta alloy, Ti-8Fe-8Ta-4Zr alloy and Ti-10Fe-10Ta-4Zr alloy, which have been developed by other researchers [39].

Figure 9 shows polarization curves of the β-Ti-18%Mo-10%Cr alloy and Ti-6%Al-4%V alloy as a reference material. Both cathodic and anodic branches on the polarization curve of the Ti-18%Mo-10%Cr alloy was lower current density than that of the Ti-6%V-4%Al alloy. The corrosion currents of the Ti-18%Mo-10%Cr alloy and the Ti-6%Al-4%V alloy were $0.61 \mu A/cm^2$ and $1.03 \mu A/cm^2$, respectively. Furthermore, it is clear that the Ti-18%Mo-10%Cr alloy shows nobler corrosion potential as compared with the Ti-6%Al-4%V alloy. Hence, the polarization investigation indicated that the newly designed Ti-18%Mo-10%Cr alloy has better corrosion resistance than commercial Ti-6%Al-4%V alloy.
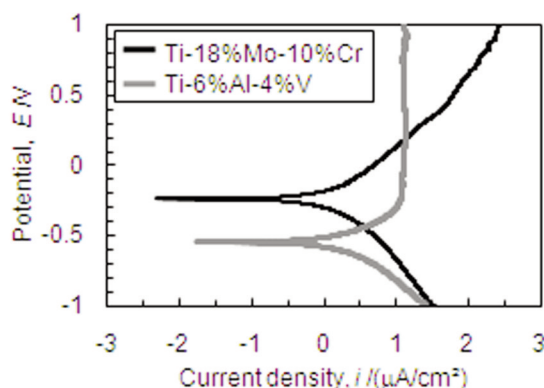
4. Conclusion

Figure 9. Relation between potential and current density of the Ti-18%Mo-10%Cr alloy and the Ti-6%Al-4%V alloy.

A new β-type Ti alloy constituted by Mo and Cr was designed and fabricated through the PM process using pure metallic powders were performed and the following findings were obtained.

1. The single β phase of Ti at ambient temperature was obtained by addition of 18%Mo and 10%Cr and by applying the PM method. The alloying behavior of pure metallic powders to their designated chemical compositions has been enhanced through sintering and solution treatment.

2. Addition of Mo and Cr increased the stability of the β phase while O promoted the formation of the α phase upon cooling. The rise in O content increased CCR for the formation of the α phase. These can be attributed to the increase in the driving force of β → α transformation and the promotion of formation of

the α phase caused by the grain-boundary segregation of O.

3. The Ti-18%Mo-10%Cr alloy exhibited almost the same hardness with other β-Ti alloys and better corrosion resistance than the commercial Ti-6%Al-4%V alloy.

References

[1] H.J. Rack, J.I. Qazi, Materials Sci. Eng., C26 (2006) 1269-1277.

[2] M. Niinomi, Met Mater Trans., 33A (2002) 477-486

[3] E.B. Taddei, V.A.R. Henriques, C.R.M. Silva, C.A.A Cairo, Mater. Sci. Eng., C24 (2004) 683-687

[4] M. Niinomi, Mater. Scie.Eng., A243 (1998) 231-236.

[5] P.J. Bania, in Beta Titanium Alloys in the 1990's (D. Eylon, R. Boyer, D. Koss), TMS, Warrendale, 1993, p. 3-24.

[6] G. Lutjering, J.C. Williams, Titanium, second ed., Springer-Verlag, Berlin, 2007, p. 30.

[7] R.M. Pilliar, in Biomedical Materials (R. Narayan), Springer Science+Business Media, New York, 2009, pp. 41-81.

[8] M. J. Donachie, Titanium Technical guide: A Technical Guide, second ed., ASM International, Ohio, 2004, p. 47.

[9] Y.G. Li, P.A. Blenkinsop, M.H. Loretto, D. Rugg, W. Voice, Acta Mater., 47 (1999) 2889-2905.

[10] E. W. Colling, in Materials properties Handbook: Titanium Alloys (R. Boyer, G. Welsch, E. W. Colling), ASM Materials Park, Ohio, 1994, p. 3-114.

[11] M. Morinaga, M. Kato, T. Kamimura, M. Fukumoto, I. Harada, K. Kubo, Proceedings of a Symposium of Titanium, June 29-July 2, San Diego, USA, 1993, p. 217-224.

[12] N. Saunders, Z. Guo, X. Li, A.P. Miodownik, J.-P. Schille´, JOM, 12 (2003) 60-65.

[13] Z. Guo, W. Sha, Mater. Sci. Eng., A 392 (2005) 449-452.

[14] M. Gomez, C.I. Garcia, D.M. Haezerbrouck and A.J. Deardo, ISIJ Intl., 49 (2009) 302-311.

[15] N. Saunders, S. Kucherenko, X. Li, A.P. Miodownik, J.-P. Schille´, J. Phas. Equi., 22 (2001) 463-469.

[16] D.A. Akinlade, W.F. Caley, N.L. Richards, M.C. Chaturvedi, Mater. Sci. Eng., A486 (2008) 626-633.

[17] M.T. Pham, I. Zyganow, W. Matz, H. Reuther, S. Oswald, E. Richter, E. Wieser, Thin Solid Films, 310 (1997) 251-259.

[18] H. Nakajima, M. Koiwa, ISIJ Intl., 31(1991) 757-766.

[19] A.V. Dobromyslov, V.A. Elkin, Scripta Mater., 44(2001) 905-910.

[20] X.H. Min, K. Tsuzaki, S. Emura, K. Tsuchiya, Mater. Sci Eng., A528 (2011) 4569-4578.

[21] Annual Book of ASTM Standard B817-08, ASM Intl.,

West Conshohocken, 1988.

[22] Z. Guo, S. Malinov, W. Sha, Comp. Mater. Sci., 32 (2005) 1-12.

[23] M.S. Oh, J.Y. Lee, J.K. Park, Metal. Mater. Trans., 35A (2004) 3071-3077.

[24] S. Takaki, K. Tsuzaki, Microstructure of Material, Asakura Shoten, Tokyo,2000, p. 100 (in Japanese).

[25] D. McLean, Grain Boundaries in Metals, Oxford University Press, 1957.

[26] M.P. Seah, E.D. Hondros, Scripta Met., 7 (1973) 735-737.

[27] S. Takaki, N. Nakada, T. Tsuchiyama in Advanced Steels: The Recent Scenario in Steel Science and Technology,(Y. Weng, H. Dong, Y. Gan) Springer, Berlin, 2011, p. 81-86.

[28] M.P. Neupane, I.S. Park, S.J. Lee, K.A. Kim, M.H. Lee, T. Sung, Int. J. Electrochem. Sci., 4 (2009) 197-207.

[29] X. Wu, J. del Prado, Q. Li, A. Huang, D. Hu, M.H. Lorretto, Acta Mater., 54 (2006) 5433-5448.

[30] Q. Wei, L. Wang, Y Fu, J. Qin, W. Lu, D. Zhang, Mater & Design, 32 (2011) 2934-2939.

[31] J.W. Martin, R.D. Doherty, B. Cantor, Stability of Microstructure in Metallic Systems, second ed., Cambridge University Press, Cambridge, 1997, p. 57.

[32] N. Wain, X.J. Hao, G.A Ravi, X. Wu, Mater. Sci. Eng., A 527 (2010) 7673-7683.

[33] M. Abdel-Hady, K. Hinoshita, M. Morinaga, Scripta Mater., 55 (2006) 477-480.

[34] F. Geng, M. Niinomi, M. Nakai, Mater. Sci. Eng, A528 (2011) 5435-5445.

[35] J.I. Qazi, B. Marquardt, H.J. Rack, JOM 11 (2004) 49.

[36] T. Saito, T. Furuta, J.H. Hwang, S. Kuramoto, K. Nishino, N. Suzuki, R. Chen, A. Yamada, K. Ito, Y. Seno, T. Nonaka, H. Ikehata, N. Nagasako, C. Iwamoto, Y. Ikuhara, T. Sakuma, Science, 300 (2003) 464-467.

[37] X. Tang, T. Ahmed and H.J. Rack, J. Mater. Sci. 35 (2000) 1805-1811.

[38] P.-J. Arrazola, A. Garay, L.-M. Iriarte, M. Armendia, S. Marya, F. Le Maître, J. Mater. Proc. Tech., 209 (2009) 2223-2230.

[39] D. Kuroda, H. Kawasaki, A. Yamamoto, S. Hiromoto and T. Hanawa, Mater. Sci. Eng., C25 (2005), p. 312-320.